Possibility of dibaryon formation near the $N^*(1440)N$ threshold: Reexamination of isoscalar single-pion production

H. Clement,[1,2,*] T. Skorodko,[1,2] and E. Doroshkevich[3]

[1]*Physikalisches Institut, Eberhard-Karls-Universität Tübingen, Auf der Morgenstelle 14, 72076 Tübingen, Germany*

[2]*Kepler Center for Astro and Particle Physics, University of Tübingen, Auf der Morgenstelle 14, 72076 Tübingen, Germany*

[3]*Institute for Nuclear Research of the Russian Academy of Sciences, Moscow, 117312, Russia*

(Received 14 July 2022; revised 24 September 2022; accepted 16 November 2022; published 15 December 2022)

The isoscalar single-pion production exhibits a broad bump in the energy dependence of the total cross section, which does not correspond to the usual opening of the $N^*(1440)$ production channel with subsequent pion decay. We reevaluate the current database and investigate whether the observed bump structure with a width of about 150 MeV points to the formation of dibaryon states with $I(J^P) = 0(1^+)$ and $0(1^-)$ near the $N^*(1440)N$ threshold. This situation would be similar to the situation at the $\Delta(1232)N$ threshold, where the signature of a number of dibaryonic resonances has been found.

DOI: 10.1103/PhysRevC.106.065204

I. INTRODUCTION

In recent years many so-called exotic states have been observed in the charmed and beauty quark sectors, both in mesons and baryons. These X, Y, Z, and pentaquark states appear as narrow resonances near particle thresholds constituting weakly bound systems of presumably molecular character [1]. In the following we discuss the corresponding situation in the unflavored dibaryon sector, which can be investigated by both elastic nucleon-nucleon (NN) scattering and NN-induced pion production. Different from the flavored sector, such dibaryonic states decay into products which usually contain unflavored excitations of the nucleon. Since those have already a large intrinsic hadronic width, such dibaryon excitations cannot be expected to be as narrow as resonances in the flavored sector, even not near thresholds, where the phase space for decay products is small.

After the recent observation of the—for a hadronic excitation—surprisingly narrow dibaryon resonance $d^*(2380)$ with $I(J^P) = 0(3^+)$ in NN scattering [2,3] and NN-induced two-pion production [4–9], new measurements and re-investigations revealed or reconfirmed evidences for various dibaryonic states near the ΔN threshold. The most pronounced resonance structure there is the one with the quantum numbers $I(J^P) = 1(2^+)$, mass $m \approx 2148$ MeV and width $\Gamma \approx 120$ MeV, which is compatible with the width of $\Delta(1232)$. Its structure in the $pp \leftrightarrow d\pi^+$ cross section coupled to the $^1D_2$ NN partial wave has been known since the 1950s. Because its mass is close to the nominal ΔN threshold of 2.17 GeV and its width is compatible with that of the Δ itself, its nature has been heavily debated in the past (see, e.g., Refs. [10–19]). Its resonance behavior has been clearly observed separately in πd [17] and pp [16] scattering as well as in the $pp \leftrightarrow d\pi^+$ reaction [15]. Also in the combined analysis of pp, πd scattering and the $pp \leftrightarrow d\pi^+$ reaction [20] the resonance effect in the $^1D_2$ pp partial wave is apparent. For a recent review about this issue see, e.g., Refs. [21,22].

Recently also evidence for a resonance with mirrored quantum numbers, i.e., $I(J^P) = 2(1^+)$, mass $m = 2140(10)$ MeV, and width $\Gamma = 110(10)$ MeV, has been published [23,24]. Due to its isospin, this resonance cannot couple directly to the NN channel. However, it can be produced associatedly in NN-induced two-pion production. It is remarkable that both these states as well as $d^*(2380)$ were predicted already in 1964 by Dyson and Xuong [25] based on $SU(6)$ multiplet considerations. More lately these states were calculated also in a Faddeev treatment by Gal and Garcilazo [26,27], providing agreement with experimental findings. These two states with mirrored quantum numbers, $I(J^P) = 1(2^+)$ and $2(1^+)$, represent weakly bound states relative to the nominal ΔN threshold and hence are of presumably molecular character with N and Δ in relative S wave—a picture supported by the Faddeev calculations of Refs. [26,27].

Recently evidence was presented for two further states, where the two baryons Δ and N are in relative P wave: a state with $I(J^P) = 1(0^-)$, $m = 2201(5)$ MeV, and $\Gamma = 91(12)$ MeV coupled to the $^3P_0$ NN partial wave as well as a state with $I(J^P) = 1(2^-)$, $m = 2197(8)$ MeV, and $\Gamma = 130(21)$ MeV coupled to the $^3P_2$ NN partial wave [28]. Whereas the values for the latter state agree with those obtained before already in SAID partial-wave analyses [20], the $I(J^P) = 1(0^-)$ state was not known before, since it is forbidden in the well-investigated two-body reaction $pp \rightleftharpoons d\pi^+$. The masses of these P-wave resonances are slightly above the nominal ΔN threshold, which is understood as being due to the additional orbital motion [28].

There is evidence for the existence of still further states like another ΔNP-wave state with $I(J^P) = 1(3^-)$, $m = 2183$ MeV, and $\Gamma = 158$ MeV coupled to the $^3F_3$ NN partial wave [20]. However, the experimental situation there is not yet as clear [21].

*heinz.clement@uni-tuebingen.de

Platonova and Kukulin demonstrated recently that both cross-section and polarization observables of the $pp \to d\pi^+$ reaction [29] as well as the participating dominant NN partial waves [30] can be described consistently on a quantitative level, if dibaryon resonances in the $^3P_2$, $^1D_2$, and $^3F_3$ NN partial waves are included. As already pointed out in previous studies [31], it is concluded that these partial waves contain both genuine resonant parts (dibaryon resonances) as well as pseudoresonant parts (due to the ΔN intermediate state).

Recent photoproduction experiments carried out at ELPH, Tohoku, and ELSA, Bonn, suggest that also at thresholds of higher-lying baryon excitations dibaryonic structures are formed [32,33]. According to their $\gamma d \to d\pi^0\pi^0$ measurements the observed structures in the so-called second and third resonance regions do not represent quasifree processes for baryon excitations, but rather constitute dibaryonic excitations at 2.47 and 2.63 GeV, respectively.

In the following we investigate whether the scenario of dibaryonic resonances near baryon excitation thresholds finds also some repetition near the $N^*(1440)N$ threshold. In a preceeding work [34] it was demonstrated that the $^1S_0$ and $^3S_1$ NN partial waves can be well described if dibaryon resonances with $I(J^P) = 1(0^+)$ and $0(1^+)$ near the N^*N threshold are postulated, for which also suggestive experimental evidence was presented. The evidences for the $I(J^P) = 0(1^+)$ state will be reconsidered in this work.

There is yet another reason to look in more detail into the isoscalar single-pion production. Recently an article [35] appeared claiming that sequential single-pion production is able to explain the $d^*(2380)$ peak in the $np \to d\pi^+\pi^-$ reaction by the particular two-step process $np(I=0) \to (pp)\pi^- \to (d\pi^+)\pi^-$. As a crucial ingredient of that work the bump structure in the isoscalar single-pion production needs to be assumed as narrow as 70 MeV, which is in conflict with the results in Refs. [36,37]. We take these claims as yet another reason to reinspect thoroughly the experimental situation in the isoscalar single-pion production.

II. EXPERIMENTAL SITUATION IN SINGLE-PION PRODUCTION

A. The purely isovector reaction $pp \to pp\pi^0$

The π^0 production in pp collisions has been measured by many groups with a number of different equipments [38–47]. Figure 1 shows the resulting total cross section from threshold up to $T_p = 1.5$ GeV ($\sqrt{s} = 2.6$ GeV). Since we are interested here mainly in the region where the cross section starts to saturate, we do not plot the energy dependence of the total cross section in logarithmic scale as is usually done, but in linear scale, in order to focus on the situation of available data in the region of interest.

Whereas the data in the near-threshold region exhibit a rather consistent behavior of a strongly increasing cross section, the available database beyond $T_p = 0.8$ GeV ($\sqrt{s} = 2.2$ GeV) displays quite some scatter in the region where the cross section starts to flatten out. There are essentially two groups of measurements, which do not coincide well within their uncertainties. The one group favors cross-section values around 4 mb; the other one favors values around 4.5 mb. The WASA-at-COSY data [36] were normalized to the average of previous measurements in this region, which is well represented by the result of Ref. [39] at $\sqrt{s} = 2.35$ GeV. The WASA-at-COSY data exhibit a flat energy dependence in the region of interest.

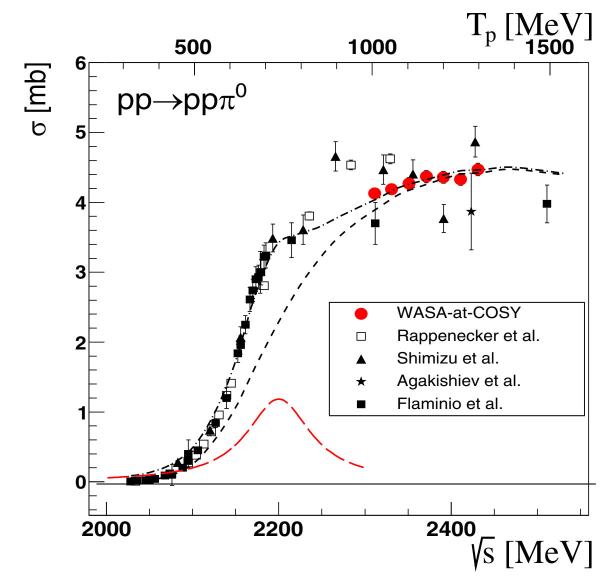

FIG. 1. Energy dependence of the total cross section for the $pp \to pp\pi^0$ reaction. Red solid circles denote the results from WASA-at-COSY [36]. Other symbols give results from earlier work [39,41–47]. The data points of Ref. [38] at $T_p = 970$ MeV and Ref. [40] at $T_p = 1480$ MeV are included in the collection of Flaminio *et al.* [47]. The short-dashed line represents a calculation for t-channel Δ and $N^*(1440)$ excitation in the framework of the Valencia model [48], rescaled by a factor of 0.98. The long-dashed curve shows a Lorentzian fitted to the data in the ΔN region representing phenomenologically the contributions from the isovector s-channel dibaryon excitations $I(J^P) = 1(0^-)$, $1(2^-)$, $1(2^+)$, and $1(3^-)$ fed by the $^3P_0$, $^3P_2$, $^1D_2$, and $^3F_3$ NN partial waves. The dash-dotted curve gives the superposition of both contributions, providing thus the full isovector cross section.

The main physics in the region of interest may be inferred from Fig. 3 of Ref. [36], where differential cross sections accumulated by the WASA-at-COSY experiment are shown over the energy region $T_p = 1.0$–1.35 GeV ($\sqrt{s} = 2.3$–2.45 GeV).

All differential distributions deviate largely from pure phase-space distributions. The $M_{p\pi^0}$ spectrum exhibits a pronounced peak resulting from the excitation of the $\Delta(1232)$ resonance in the course of the reaction process. The strongly anisotropic proton angular distribution is in accord with a peripheral reaction process and the also anisotropic pion angular distribution may be associated with the p-wave decay of the Δ excitation.

In a reanalysis of the WASA-at-COSY data [36] we confirm the published differential cross sections within their quoted uncertainties, so there is no need to show them here again. Instead we show the Dalitz plot of the pp-invariant mass squared, M_{pp}^2, versus the $p\pi^0$-invariant mass squared,

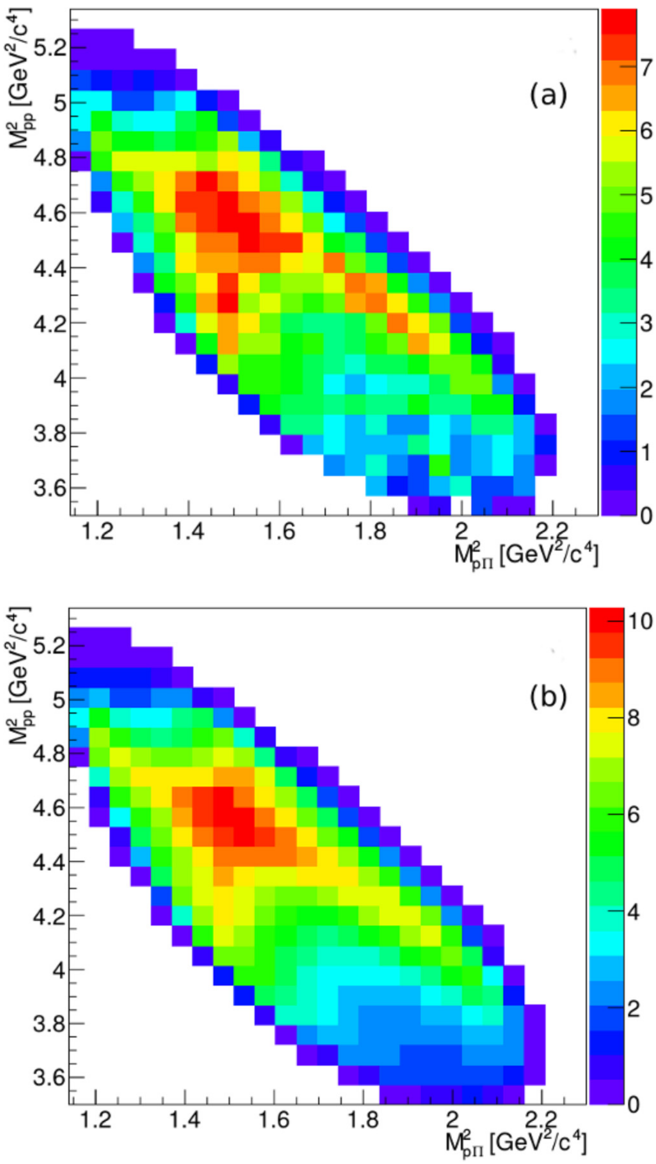

FIG. 2. Dalitz plot of the pp-invariant mass squared, M^2_{pp}, versus the $p\pi^0$-invariant mass squared, $M^2_{p\pi^0}$, for the energy bin $\sqrt{s} = 2.40$–2.42 GeV of the $pp \to pp\pi^0$ reaction. On the top the data from our reanalysis are shown and on the bottom a model calculation for Δ excitation is displayed. The intensity distribution is color coded in the usual way in a linear scale with violet and red colors denoting the lowest and the highest intensities, respectively.

$M^2_{p\pi^0}$, in Fig. 2. The data from our reanalysis are shown on the top and a model calculation for Δ excitation is displayed on the bottom. In both data and calculation the vertical band for Δ excitation is clearly seen as well as its reflection due to the fact that we have two identical protons, where the Δ excitation can happen in either one.

All data are very well described by assuming just Δ excitation in the reaction process. Inclusion of a small Roper contribution does not change the fit to the data noticeably. But the fit to the data starts to deteriorate markedly if the Roper contribution exceeds 0.4 mb in the total cross section. This finding may serve us as an upper limit for the isovector Roper contribution in the $pp \to pp\pi^0$ reaction. We note that the observations in the differential spectra from WASA-at-COSY are consistent with those obtained in Refs. [42,44] at lower energies.

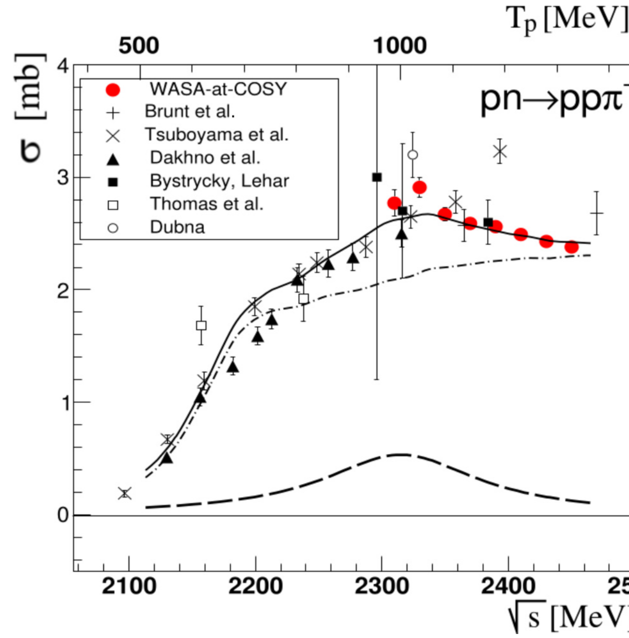

FIG. 3. Energy dependence of the total cross section in dependence for the $pn \to pp\pi^-$ reaction. Red solid circles denote the results from WASA-at-COSY [36]. Other symbols give results from earlier work [41,49–52,54]. The dash-dotted line gives the purely isovector contribution obtained by the dash-dotted line in Fig. 1 with the absolute scale being reduced by a factor of 2. Adding the Lorentzian from Fig. 6 (dashed curve)—divided by a factor of 3 for the representation of the isoscalar contribution in this channel—results in the solid curve.

B. The isospin-mixed reaction $pn \to pp\pi^-$

For this reaction there are much fewer measurements due to the need for an effective neutron beam or target. Some experiments were conducted by utilizing the quasifree reaction process in the collision of deuterons with protons by using either a deuteron beam hitting a hydrogen bubble chamber [49] or a proton beam hitting a deuteron bubble chamber [50,51]. The measurements of Refs. [49,50] are over a wide energy range; their resulting cross sections are in good agreement with each other in the overlap region.

Other experiments used a dedicated neutron beam produced in a first scattering process by proton collisions on a deuteron target, where the produced neutron beam was directed either on a hydrogen bubble chamber [44] or on a liquid hydrogen target [52,53]. In the latter the isospin-mirrored reaction $np \to nn\pi^+$ was measured in the near-threshold region.

The total cross sections obtained in the measurements are shown in Fig. 3 in linear scale. There is good agreement between the WASA-at-COSY measurements [36] and previous results from Refs. [41,49–51] with the exception of the data

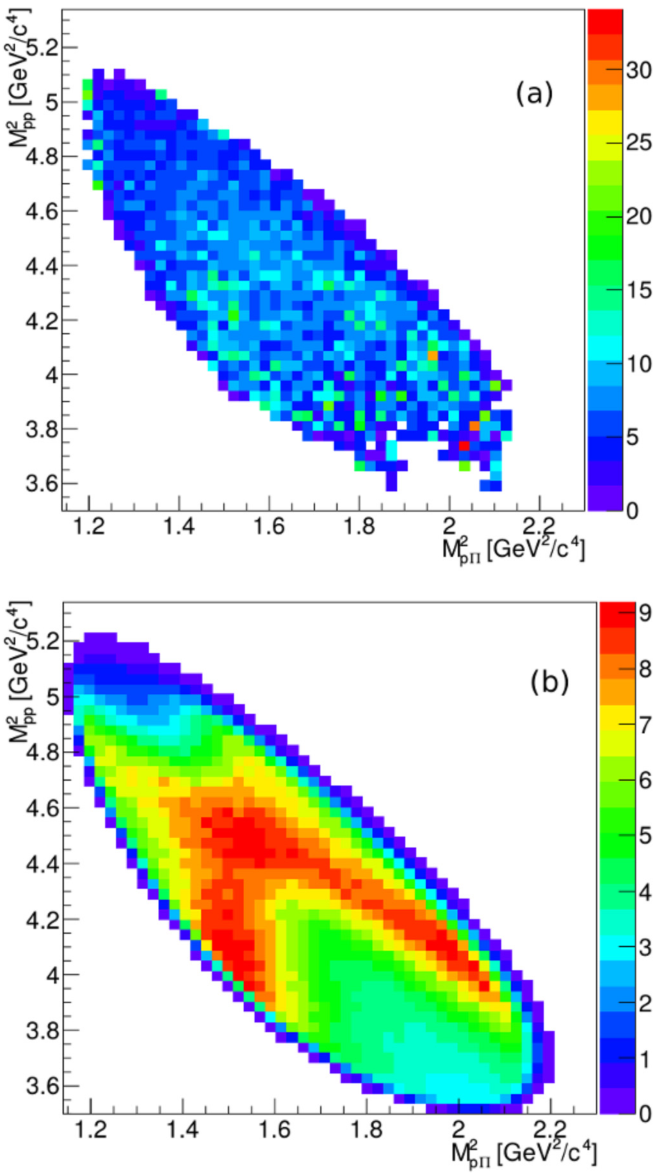

FIG. 4. Dalitz plot of the pp-invariant mass squared, M^2_{pp}, versus the $p\pi^-$-invariant mass squared, $M^2_{p\pi^-}$, for the energy bin $\sqrt{s} =$ 2.40–2.42 GeV of the $pn \to pp\pi^-$ reaction. On the top the data from our reanalysis are shown and on the bottom a model calculation for Δ and Roper excitations is displayed. The intensity distribution is color coded in the usual way in a linear scale with violet and red colors denoting the lowest and the highest intensities, respectively.

point at $T_P = 1.17$ GeV ($\sqrt{s} = 2390$ MeV) from Ref. [49], which is far off from the other experimental results.

As demonstrated in Ref. [36] the differential distributions of the $pn \to pp\pi^-$ reaction can no longer be described by just the Δ excitation, but necessitate also a substantial Roper excitation. This is also borne out in the Dalitz plot displayed in Fig. 4 for the $pn \to pp\pi^-$ reaction.

C. The isoscalar single-pion production

The isoscalar part of the NN-induced single-pion production cannot be measured directly. It rather has to be deduced from a combination of various single-pion production measurements. Most common is the comparison of the total cross sections for the $pp \to pp\pi^0$ and $np \to pp\pi^-$ reaction channels by assuming isospin invariance:

$$\sigma_{pn\to NN\pi}(I=0) = \tfrac{3}{2}(2\sigma_{pn\to pp\pi^-} - \sigma_{pp\to pp\pi^0}), \qquad (1)$$

where $\sigma_{pn\to NN\pi}(I=0)$ denotes the isoscalar np-induced single-pion production cross section [37,41,50]. Results obtained by use of this method are shown in Fig. 5 by solid dots [36], solid triangles [50], solid squares [42], and open triangles [45].

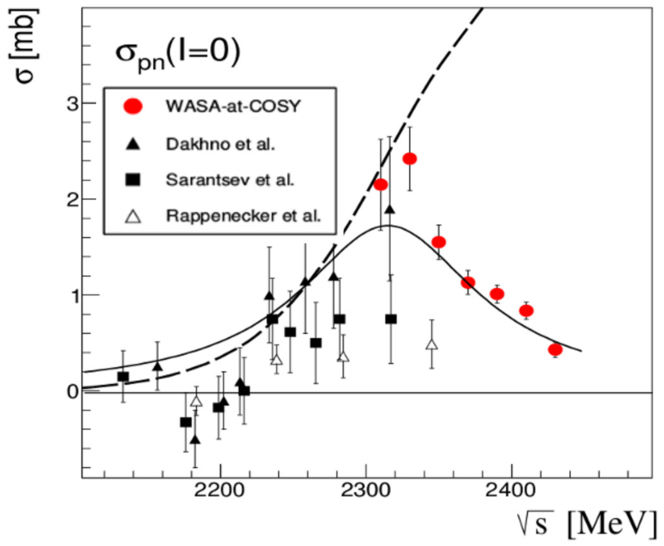

FIG. 5. The pn-induced isoscalar single-pion production cross section based on Eq. (1) in dependence of the total c.m. energy $\sqrt{s}$. Shown are the recent results from WASA-at-COSY [36,37] (solid circles) together with earlier results from Ref. [50] (solid triangles), Ref. [42] (solid squares), and Ref. [45] (open triangles). The dashed line shows the expected energy dependence based on t-channel Roper excitation [48] adjusted in height arbitrarily to the data point at $\sqrt{s} = 2260$ MeV. The solid line represents a Lorentzian with $m = 2315$ MeV and $\Gamma = 150$ MeV.

Since we have the difference of two nearly equally sized values in Eq. (1), the relative uncertainty in the absolute normalization of the two cross-section values leads to a large uncertainty in the resulting isoscalar cross section. This explains also the large scatter in the obtained results. Nevertheless, all data are consistent with an increasing cross section from threshold up to $\sqrt{s} \approx 2300$ MeV and leveling off there. The WASA-at-COSY data show that the cross section starts falling at subsequent higher energies.

An alternative to this difference method given by Eq. (1) has been employed in Ref. [44]. There all differential distributions obtained in bubble-chamber measurements of the $pp \to pp\pi^0$ and $np \to pp\pi^-$ reactions have been subjected to a partial-wave analysis (PWA). The interference between isovector and isoscalar amplitudes as it shows up in differential cross sections, in particular in angular distributions, provides a discrimination between isoscalar and isovector

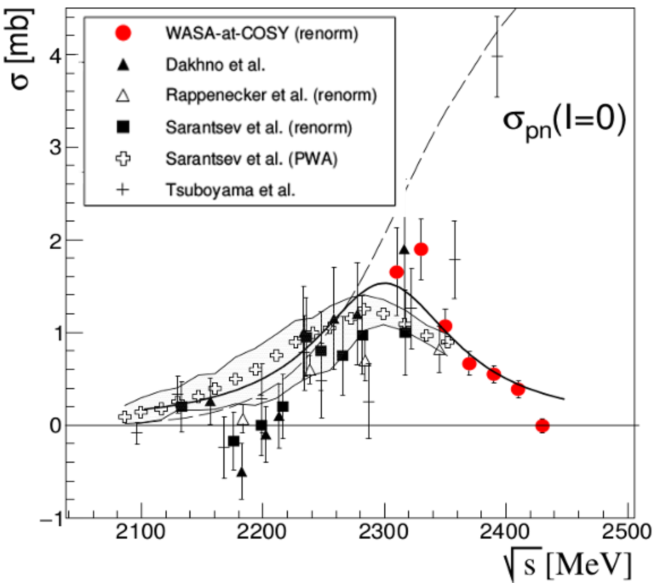

FIG. 6. The same as Fig. 5, but with renormalized results from WASA-at-COSY [36,37] and Refs. [42,45] (see text), and the PWA results of Ref. [44] (open crosses with hatched band). The solid line represents a Lorentzian fit with $m = 2310$ MeV and $\Gamma = 150$ MeV. The dashed line shows the expected energy dependence based on t-channel Roper excitation [36,48] adjusted in height arbitrarily to the data point at $\sqrt{s} = 2260$ MeV.

contributions in the partial-wave analysis. Hence the results of this work appear to be particularly reliable. They are given in Fig. 6 by the hatched band, where the bandwidth denotes the uncertainty of that analysis. The band rises with rising energy reaching a peak around $\sqrt{s} \approx 2.30$ GeV and starts falling in height thereafter. This latter feature agrees with the trend observed in the WASA-at-COSY data [36], only that the WASA-at-COSY values are higher by about 30% in the overlap region, which, however, is well within their uncertainty in absolute scale [36].

In the following we show that the large scatter in the experimental results for $\sigma_{pn}(I=0)$ can be easily cured by a slight renormalization of the various data samples well within their quoted uncertainties. Inspection of Eq. (1) shows that an uncertainty $\delta\sigma$ in the absolute magnitude of the $pp \to pp\pi^-$ cross section relative to that of the $pn \to pp\pi^0$ cross section enters linearly in Eq. (1) by a term $3\delta\sigma = 3\sigma_{pn\to pp\pi^-}(\delta\sigma/\sigma_{pn\to pp\pi^-})$, which causes essentially a baseline shift in the deduced data for $\sigma_{pn\to NN\pi}(I=0)$ in the region where $pp \to pp\pi^0$ and $pn \to pp\pi^-$ cross sections level off. So already a 1% change in the normalization of $\sigma_{pn\to pp\pi^-}$, i.e., $\delta\sigma/\sigma_{pn\to pp\pi^-} = 1\%$, leads to a shift of $\sigma_{pn\to NN\pi}(I=0)$ by $3\delta\sigma \approx 0.08$ mb for $\sqrt{s} > 2.25$ GeV. Hence, in order to achieve agreement between PWA and WASA-at-COSY results it suffices to change the relative normalization between $pp \to pp\pi^0$ and $pn \to pp\pi^-$ cross sections of the WASA data by 4%, leading to a shift of about 0.3 mb. Such a renormalization of the WASA results is well within the uncertainty of 7% in the relative normalization between $pp \to pp\pi^0$ and $pn \to pp\pi^-$ cross sections quoted in Ref. [36]. Similarly, we may obtain reasonable overlap of the PWA results with those of Refs. [42] and [45], if we renormalize those by 3% and 4%, respectively, in their relative normalization between $pp \to pp\pi^0$ and $pn \to pp\pi^-$ cross sections. Again, this is well within the uncertainties there. In particular we see that by such a renormalization the results of Ref. [42] get in practical perfect overlap with the uncertainty band of the PWA results [44].

The renormalized data of Refs. [42,45] and WASA-at-COSY [36] are compared with the PWA results in Fig. 6, where they exhibit now a very consistent structure of an isoscalar cross section rising from threshold up to about 2.3 GeV and declining thereafter. This structure can be well described by a Breit-Wigner shape having a width of 150(20) MeV and peaking at 2.31(1) GeV—in accordance with the results reported in Refs. [34,36]. Also the results from Refs. [49,50] fit reasonably well, without any need for renormalization. Only the highest energy point from Ref. [49] at $\sqrt{s} = 2390$ MeV is far away from the trend of the other data. The reason for this lies in the much too large cross section $\sigma_{pn\to pp\pi^-}$ obtained by Ref. [49] at that energy (see Fig. 3).

To visualize how this bell-shaped isoscalar cross section evolves, we inspect again Figs. 1 and 3, the energy excitation function of the $pp \to pp\pi^0$ and $pn \to pp\pi^-$ cross sections, where the isoscalar part originates from. These cross sections are connected by the isospin relation given in Eq. (1), where $\sigma(pp \to pp\pi^0)$ is a purely isovector contribution of NN-induced single-pion production. The Valencia model calculations for t-channel Δ excitation reproduce this isovector contribution very well for incident energies $T_p > 1$ GeV—both in total (short-dashed line in Fig. 1) and differential cross sections (Fig. 3 of Ref. [36]). In the region $T_p = 0.5$–1.0 GeV, however, the calculated cross sections come out much too low. This is understandable, since these calculations do not include the isovector ΔN dibaryon excitations with $I(J^P) = 1(0^-)$, $1(2^-)$, $1(2^+)$, and $1(3^-)$ fed by the $^3P_0$, $^3P_2$, $^1D_2$, and $^3F_3$ pp partial waves in an s-channel resonance process. Among these $^3P_2$ gives the by far largest contribution to the $pp \to pp\pi^0$ cross section [44].

Here we are interested just in a simple pragmatic description of the isovector single-pion production cross section for application in Eq. (1). Hence we represent these isovector dibaryon excitations conveniently by a Lorentzian centered at $\sqrt{s} = 2200$ MeV with a width of 90 MeV and a height of about 1 mb (long-dashed curve in Fig. 1), in order to obtain a reasonable description of the $pp \to pp\pi^0$ cross section.[1] Adding up both contributions gives the dash-dotted curve in Fig. 1, which provides a very reasonable phenomenological representation of the isovector single-pion production in the $pp\pi^0$ channel.

[1]According to Ref. [44] the $^3P_2$ partial wave provides the by far largest contribution to the total cross section with about 1.5 mb. According to Ref. [29] not all of the partial wave contribution leads to s-channel dibaryon formation. Hence a total dibaryon resonance contribution of 1 mb appears to be at least qualitatively quite reasonable.

Next we consider the $pp\pi^-$ channel, which is isospin mixed. Its isovector part is given by half of the $pp \to pp\pi^0$ cross section as illustrated in Fig. 3 by the dash-dotted line. It describes the data in this channel reasonably up to $\sqrt{s} \approx$ 2.2 GeV. Beyond this energy the data exhibit a bell-shaped surplus of cross section, which has to be purely isoscalar according to Eq. (1) and which is well accounted for by the Lorentzian obtained by the fit to the full isoscalar *pn*-initiated single-pion production cross section displayed in Fig. 6.

To learn more details about the nature of the bump structure in the isoscalar cross section, we refer to Fig. 6 of Ref. [36], where the isoscalar $N\pi$-invariant mass spectrum is shown. It exhibits essentially a single pronounced structure, which peaks at $m \approx$ 1370 MeV revealing a width of $\approx$150 MeV. This structure emerges well above the isovector Δ excitation (which is filtered out by the isospin condition) and is located already in the region of the Roper excitation.

III. THE ROPER EXCITATION IN *NN*-INDUCED SINGLE-PION PRODUCTION AND THE ISSUE OF POSSIBLE N^*N STATES

Ever since its first detection by Roper in 1964 [55] the $N^*(1440)$ resonance has been heavily debated concerning its nature. The finding that it is in principle of a two-pole nature [56] increases its complexity discussed in many subsequent studies [57–60].

In contrast to the Δ excitation, the Roper excitation $N^*(1440)$ in general does not produce very eye-catching structures in hadronic reactions. Usually it appears quite hidden in the observables and in most cases can be extracted from the data only by sophisticated analysis tools like partial-wave decomposition. An exception appears here the *pn*-induced isoscalar single-pion production, where it can be observed free of the usually overwhelming isovector Δ excitation.

The extracted values for mass and width of the structure observed in the isoscalar nucleon-pion invariant-mass spectrum (Fig. 6 of Ref. [36]) appear to be compatible with the pole values for the Roper resonance deduced in diverse πN and γN studies [61]. Our values for the Roper peak are in reasonable agreement, too, with earlier findings from hadronic $J/\psi \to \bar{N}N\pi$ decay [62] and αN scattering [63,64]. However, our values deviate substantially from its Breit-Wigner values, which for the Roper resonance is quite different and which should be the standard to compare with. With regard to its Breit-Wigner mass the Roper resonance appears here to be bound by about 70 MeV within the N^*N system. Such a binding then also explains naturally its observed reduced width of 150 MeV, since the Roper width is strongly momentum dependent due to its $N\pi$ *p*-wave nature.

Since at threshold the conventional *t*-channel Roper excitation can be expected to be produced in *S* wave relative to the other nucleon and since the pion from the Roper decay is emitted in relative *p* wave, we would conventionally expect a threshold behavior for the energy dependence of the $pn \to (NN\pi)_{I=0}$ cross section like that for pion *p* waves as borne out by the calculations for *t*-channel Roper excitation in the framework of the modified Valencia model [36,48]—in Figs. 5 and 6 arbitrarily adjusted in height to the data point at $\sqrt{s} \approx 2260$ MeV and displayed by the dashed line. The data presented there follow this expectation by exhibiting an increasing cross section with increasing energy up to about $\sqrt{s} \approx 2.30$ GeV. Beyond that, however, the data fall in cross section in sharp contrast to the expectation for a *t*-channel production process. The observed behavior rather is in agreement with an *s*-channel resonance process as expected for the formation of a dibaryonic state near the N^*N threshold.

If we combine this dibaryon hypothesis with the result of the partial-wave analysis [44] for the isoscalar single-pion production, then the observed bump structure must consist actually of two resonances: one resonance where N and N^* are in relative *S* wave, yielding $I(J^P) = 0(1^+)$ and connected to the coupled ${}^3S_1$–${}^3D_1$ *np* partial waves, and one resonance where N and N^* are in relative *P* wave, yielding $I(J^P) = 0(1^-)$ and connected to the ${}^1P_1$ partial wave. At first glance it might not appear very convincing that two resonances sit practically on top of each other and produce thus just a single resonancelike structure in the total cross section. But exactly such a scenario is observed also near the ΔN threshold, where the isovector 0^-, 2^+, 2^-, and 3^- states happen to have similar masses with mass differences small compared to their width. And since the width of the N^*N states is still substantially larger than that of the ΔN states, small mass differences are washed out in the summed shape. We note that 1^+ and 1^- constitute the only possible J^P combinations for isoscalar *S* and *P* waves.

In the following we examine whether this dibaryon hypothesis leads to any conflicts with regard to unitarity, decay properties, and poles in elastic *np* scattering.

A. Relation to isoscalar two-pion production

Since the Roper resonance decays in addition via two-pion emission, the same should be valid also for the N^*N configuration. Indeed, there is an indication of such a decay in the $pn \to d\pi^0\pi^0$ reaction, which might solve another puzzling problem. Whereas the data for this reaction can be reasonably well described by a simple Breit-Wigner ansatz with momentum-independent widths, the description worsens on the low-energy side, if we apply a sophisticated momentum-dependent ansatz for the widths [65].

The situation is shown in Fig. 7, where the energy dependence of the total cross section for the $pn \to d\pi^0\pi^0$ reaction is plotted. Since the conventional background of *t*-channel processes is particularly low in this reaction channel, it is, so to speak, the "golden" channel for the observation of the $d^*(2380)$ dibaryon resonance. The solid line represents the calculated d^* excitation taking into account the momentum dependence of its width in great detail [65]. This theoretical curve describes the data very well except in the low-energy tail of $d^*(2380)$ around $\sqrt{s} = 2.3$ GeV, where it clearly underpredicts the data. If we plot the difference between data and calculation by the (black) solid dots in Fig. 7, then we note a bell-shaped distribution, the right-hand side of which is strongly dependent on the details (mass, width) of the $d^*(2380)$ resonance curve. Associating this distribution with a contribution from the possible N^*N structure we can deduce a peak cross section of roughly 25 μb at 2.3 GeV for its two-pion

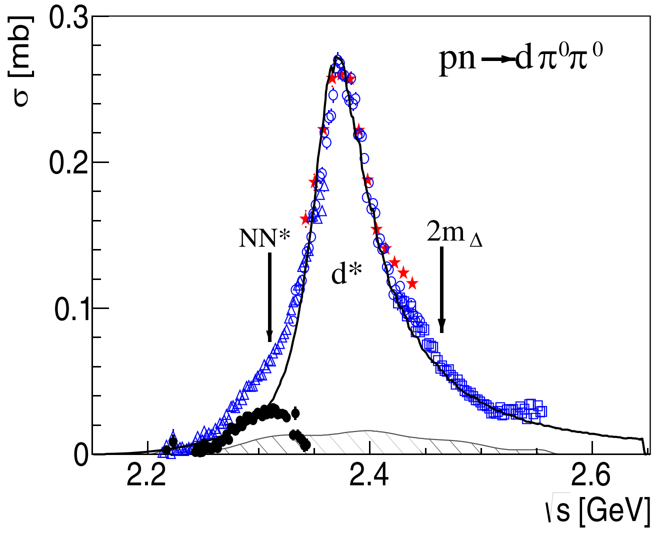

FIG. 7. Energy dependence of the total cross section for the $pn \to d\pi^0\pi^0$ reaction as measured by WASA-at-COSY. The blue open symbols represent the data of Ref. [5] normalized to the data (red stars) of Ref. [6]. The hatched area gives an estimate of systematic uncertainties. The solid curve displays a calculation of the d^* resonance with momentum-dependent widths [65]. It includes both Roper and $\Delta\Delta$ t-channel excitations as background reactions. The black solid dots show the difference between data and this calculation in the low-energy tail of $d^*(2380)$.

decay into the $d\pi^0\pi^0$ channel. Consequently we expect a contribution of such a two-pion decay of the N^*N system also in the other two-pion production channels with isoscalar contribution, which are the channels $d\pi^+\pi^-$, $pn\pi^+\pi^-$, and $pn\pi^0\pi^0$. By isospin relations the isoscalar Roper contribution in the first two reactions is twice that in each of the channels $d\pi^0\pi^0$ and $pn\pi^0\pi^0$. Here we also assume that the branching into $d\pi^+\pi^-$ ($d\pi^0\pi^0$) and $pn\pi^+\pi^-$ ($pn\pi^0\pi^0$) channels is essentially identical—as is the case for $d^*(2380)$ [66–68]. Altogether these contributions add then up to a total of roughly 150 μb.

In the two-pion decay of the N^*N systems with $J^P = 1^+$ the emitted particles are in relative s wave to each other. In the case of $J^P = 1^-$ the pions are in p wave relative to the deuteron. Both contributions appear summed up in the angular distributions for deuterons and pions. Hence we expect only mildly curved angular distributions, which actually agrees with the observations for $\sqrt{s} < 2.34$ GeV, where the $d^*(2380)$ contribution is still small [69].

B. Branching ratios of putative N^*N resonances

Having identified all inelastic decay channels we can extract now the branching ratios for $(N^*N)_{I(J^P)=0(1^+)} \to NN$, $NN\pi$, and $NN\pi\pi$ in analogy to what was done for $d^*(2380)$ [66].

For a $J = 1$ resonance formed in pn collisions at 2315 MeV the unitarity limit is given by [66]

$$\sigma_0 = \frac{4\pi}{k_i^2}\frac{2J+1}{(2s_p+1)(2s_n+1)} = 8 \text{ mb}, \tag{2}$$

where k_i, s_p, and s_n denote the initial center-of-mass momentum, and the proton and the neutron spin, respectively. The branching ratio for the decay into the elastic channel, $BR_i = \Gamma_i/\Gamma$ with Γ_i and Γ denoting the decay widths into the initial channel and the total width, respectively, is then given by [66]

$$BR_i = \frac{1}{2} - \sqrt{\frac{1}{4} - \frac{\sigma_{pn\to N^*N}(peak)}{\sigma_0}}. \tag{3}$$

From the partial-wave analysis of Ref. [44] we infer that about 25% (75%) of $\sigma_{pn\to NN\pi}(I=0)$ contributes to the 1^+ (1^-) state with a peak cross section of 0.3 (1.0) mb. This leads then in Eq. (3) to $BR_i(1^+) = 0.04(2)$ and $BR_i(1^-) = 0.15(3)$, respectively. The branchings into $NN\pi$ and $NN\pi\pi$ channels are then 85(10)% and 11(2)%, respectively, for the 1^+ state. For the 1^- state these numbers get 75(15)% and 10(2)%, respectively. The estimated uncertainties quoted in parentheses include those from the partial-wave analysis and a 20% uncertainty in the absolute scale of the isoscalar cross section.

Recently Kukulin *et al.* [34] have predicted a $I(J^P) = 0(1^+)$ resonance based on the analysis of the $^3S_1$ NN-partial wave within the dibaryon-based NN-interaction model [30,70], where also a short preview of this work was provided. The Argand plot of the calculated $^3S_1$ partial wave (Fig. 6 in Ref. [34]) shows a resonance circle with diameter of about 0.09, which according to Höhler [71] corresponds just to the elastic branching ratio BR_i. Though this value means already a very small elasticity, it is still somewhat larger than we obtain here.

C. Poles of N^*N resonances in elastic np scattering

In principle, the poles of such N^*N resonances should be sensed in partial-wave analyses of elastic np scattering. At a first glance, the situation appears to be similar to that for the meanwhile established dibaryon resonance $d^*(2380)$, where only the measurement of the analyzing power of pn scattering in the region of this resonance could reveal its pole in the $^3D_3-^3G_3$ coupled partial waves [2,3,72]. Due to their large angular momenta these partial waves have a large impact on the analyzing power. And since the analyzing power consists of just interference terms, this observable is very suitable to reveal substantial effects even from small resonance admixtures in partial waves. In the case of the $I(J^P) = 0(1^+)$ resonance candidate we deal here with an S-wave resonance, which makes no contribution to the analyzing power. Hence this key observable for revealing small contributions from resonances is not working here. In addition, the large total width of these N^*N resonances combined with a small elasticity BR_i increase the difficulty to reveal their poles by elastic scattering. Even the dedicated dibaryon search by high-resolution energy scans of pp elastic scattering with the EDDA detector at COSY was restricted to the search of narrow resonances only [73].

Though it seems that we have no suitable handle to reveal the pole of such an S-wave resonance by partial-wave analyses of elastic scattering data, their imprint on the $^3S_1$ partial wave due to intermediate dibaryon formation in the s-channel NN interaction has been shown to be significant. In Ref. [34] it was demonstrated that this resonance leads to a quantitative reproduction of the empirical values for coupled ${}^3S_1-{}^3D_1$ partial waves up to 1 GeV obtained in SAID partial-wave analyses [74]. Conversely, the successful description of these partial waves also means that our finding about this resonance is not in conflict with elastic scattering data.

For the $I(J^P) = 0(1^-)$ state the situation appears perhaps a bit more promising. It is true that again the large width of this state hampers any detection of its resonance signal in elastic pn scattering enormously, but its increased elastic branching of about 15% is in favor of a better sensible signal there. Unfortunately the SAID single-energy solutions stop at 1.1 GeV and hence cover only the low-energy tail of this resonance candidate.

IV. CONCLUSIONS

We have reanalyzed the situation of NN-induced isoscalar single-pion production. The total cross-section data exhibit a bumplike energy dependence, which can be described by a Lorentzian with mass 2310 MeV and width of about 150 MeV. This is at variance with a width as narrow as 70 MeV assumed in Ref. [35].

The fact that the observed isoscalar $M_{N\pi}$ spectrum accumulates most of its strength in the region of the Roper resonance suggests that the observed bump is of N^*N nature. Taking into account the results of the partial-wave analysis of Ref. [44], this resonancelike structure contains actually two isoscalar resonances, one with $J^P = 1^+$ and the other one with $J^P = 1^-$. These are also the only two possibilities to form resonances in isoscalar S- and P-wave NN scattering. The situation appears similar to the one observed near the ΔN threshold where several resonances have been found, which all have similar mass and width.

From the energy dependence of NN-induced isoscalar single-pion and isovector double-pion production we see that both isospin-spin combinations in the $N^*(1440)N$ system lead possibly to dibaryonic states in the Roper excitation region—analogous to the situation at the Δ threshold. However, compared to the situation there the Roper excitation cross sections discussed here are small. Also, since these structures decay mainly into inelastic channels, their poles are hard to be sensed in partial-wave analyses of elastic scattering. Nevertheless, their effect on the ${}^3S_1$ and ${}^1P_1$ NN partial waves has been shown to be important in the NN-interaction model of Kukulin *et al.*, where the short-range part of the NN interaction is represented by s-channel dibaryon formation in the various low-L partial waves [30,34,70] based on ideas given in Ref. [75].

Note added. In a recent publication [76] it was demonstrated that real and imaginary parts of the ${}^1P_1$ partial-wave amplitude derived [74] from elastic scattering data can be very well described by the NN-interaction model of Kukulin *et al.*, if a dibaryon resonance is included in this partial wave with mass and width compatible with the values deduced in this work.

ACKNOWLEDGMENTS

We are indebted to V. Kukulin[2] and M. Platonova for valuable discussions and to L. Alvarez-Ruso for using his code. We acknowledge valuable discussions with E. Oset, A. Gal, and I. Strakovsky. This work has been supported by DFG (CL 214/3-3).

[2]Deceased.

[1] F.-K. Guo, C. Hanhart, Ulf-G. Meiβner, Q. Wang, Q. Zhao, and B.-S. Zou, Rev. Mod. Phys. **90**, 015004 (2018).
[2] P. Adlarson *et al.*, Phys. Rev. Lett. **112**, 202301 (2014).
[3] P. Adlarson *et al.*, Phys. Rev. C **90**, 035204 (2014).
[4] M. Bashkanov *et al.*, Phys. Rev. Lett. **102**, 052301 (2009).
[5] P. Adlarson *et al.*, Phys. Rev. Lett. **106**, 242302 (2011).
[6] P. Adlarson *et al.*, Phys. Lett. B **721**, 229 (2013).
[7] P. Adlarson *et al.*, Phys. Rev. C **88**, 055208 (2013).
[8] P. Adlarson *et al.*, Phys. Lett. B **743**, 325 (2015).
[9] H. Clement, M. Bashkanov, and T. Skorodko, Phys. Scr. T **166**, 014016 (2015).
[10] R. L. Shypit, D. V. Bugg, D. M. Lee, M. W. McNaughton, R. R. Silbar, N. M. Stewart, A. S. Clough, C. L. Hollas, K. H. McNaughton, P. Riley, and C. A. Davis, Phys. Rev. Lett. **60**, 901 (1988).
[11] R. L. Shypit, D. V. Bugg, A. H. Sanjari, D. M. Lee, M. W. McNaughton, R. R. Silbar, C. L. Hollas, K. H. McNaughton, P. Riley, and C. A. Davis, Phys. Rev. C **40**, 2203 (1989).
[12] M. G. Ryskin and I. I. Strakovsky, Phys. Rev. Lett. **61**, 2384 (1988).
[13] A. V. Kravtsov, M. G. Ryskin, and I. I. Strakovsky, J. Phys. G **9**, L187 (1983).
[14] I. I. Strakovsky, A. V. Kravtsov, and M. G. Ryskin, Yad. Fiz. **40**, 429 (1984) [Sov. J. Nucl. Phys. **40**, 273 (1984)].
[15] R. A. Arndt, I. I. Strakovsky, R. L. Workman, and D. V. Bugg, Phys. Rev. C **48**, 1926 (1993).
[16] R. A. Arndt, I. I. Strakovsky, and R. L. Workman, Phys. Rev. C **50**, 2731 (1994).
[17] R. A. Arndt, I. I. Strakovsky, and R. L. Workman, Phys. Rev. C **50**, 1796 (1994).
[18] N. Hoshizaki, Phys. Rev. C **45**, R1424 (1992).
[19] N. Hoshizaki, Prog. Theor. Phys. **89**, 245 (1993); **89**, 251 (1993); **89**, 563 (1993); **89**, 569 (1993).
[20] Ch. H. Oh, R. A. Arndt, I. I. Strakovsky, and R. L. Workman, Phys. Rev. C **56**, 635 (1997), and references therein.
[21] H. Clement, Prog. Part. Nucl. Phys. **93**, 195 (2017).
[22] H. Clement and T. Skorodko, Chin. Phys. C **45**, 022001 (2021).
[23] P. Adlarson *et al.*, Phys. Rev. Lett. **121**, 052001 (2018).
[24] P. Adlarson *et al.*, Phys. Rev. C **99**, 025201 (2019).
[25] F. J. Dyson and N.-H. Xuong, Phys. Rev. Lett. **13**, 815 (1964).
[26] A. Gal and H. Garcilazo, Nucl. Phys. A **928**, 73 (2014).

[27] A. Gal, Phys. Lett. B **769**, 436 (2017).
[28] V. Komarov *et al.*, Phys. Rev. C **93**, 065206 (2016).
[29] M. N. Platonova and V. I. Kukulin, Phys. Rev. D **94**, 054039 (2016).
[30] V. I. Kukulin, V. N. Pomerantsev, O. A. Rubtsova, and M. N. Platonova, Phys. At. Nucl. **82**, 934 (2019).
[31] I. I. Strakovsky, Fiz. Elem. Chast. Atom. Yadra **22**, 615 (1991) [Sov. J. Part. Nucl. **22**, 296 (1991)], and references therein.
[32] T. Ishikawa *et al.*, Phys. Lett. B **772**, 398 (2017).
[33] T. C. Jude *et al.*, Phys. Lett. B **832**, 137277 (2022).
[34] V. I. Kukulin, O. A. Rubtsova, M. N. Platonova, V. N. Pomerantsev, H. Clement, and T. Skorodko, Eur. Phys. J. A **56**, 229 (2020).
[35] R. Molina, N. Ikeno, and E. Oset, arXiv:2102.0557.
[36] P. Adlarson *et al.*, Phys. Lett. B **774**, 599 (2017).
[37] P. Adlarson *et al.*, Phys. Lett. B **806**, 135555 (2020).
[38] D. V. Bugg *et al.*, Phys. Rev. **133**, B1017 (1964).
[39] F. Shimizu *et al.*, Nucl. Phys. A **386**, 571 (1982).
[40] A. M. Eisner *et al.*, Phys. Rev. **138**, B670 (1965).
[41] J. Bystricky *et al.*, J. Phys. **48**, 1901 (1987), and references therein.
[42] V. V. Sarantsev *et al.*, Eur. Phys. J. A **21**, 303 (2004).
[43] K. N. Ermakov *et al.*, Eur. Phys. J. A **47**, 159 (2011).
[44] V. V. Sarantsev *et al.*, Eur. Phys. J. A **43**, 11 (2010).
[45] G. Rappenecker *et al.*, Nucl. Phys. A **590**, 763 (1995), and references therein.
[46] G. Agakishiev *et al.*, Eur. Phys. J. A **51**, 137 (2015).
[47] V. Flaminio *et al.*, CERN libraries, CERN-HERA Report No. 84-01 (1984).
[48] L. Alvarez-Ruso, E. Oset, and E. Hernandez, Nucl. Phys. A **633**, 519 (1998); (private communication).
[49] T. Tsuboyama, N. Katayama, F. Sai, and S. S. Yamamoto, Nucl. Phys. A **486**, 669 (1988).
[50] L. G. Dakhno *et al.*, Phys. Lett. B **114**, 409 (1982).
[51] D. C. Brunt, M. J. Clayton, and B. A. Westwood, Phys. Rev. **187**, 1856 (1969).
[52] W. Thomas *et al.*, Phys. Rev. D **24**, 1736 (1981).
[53] M. Kleinschmidt *et al.*, Z. Phys. A **298**, 253 (1980).
[54] A. Abdivaliev *et al.* (unpublished).
[55] L. D. Roper, Phys. Rev. Lett. **12**, 340 (1964).
[56] R. A. Arndt, J. M. Ford, and L. D. Roper, Phys. Rev. D **32**, 1085 (1985).
[57] R. E. Cutkosky and S. Wang, Phys. Rev. D **42**, 235 (1990).
[58] R. A. Arndt, W. J. Briscoe, I. I. Strakovsky, and R. L. Workman, Phys. Rev. C **74**, 045205 (2006).
[59] M. Döring *et al.*, Nucl. Phys. A **829**, 170 (2009).
[60] N. Suzuki, B. Juliá-Díaz, H. Kamano, T.-S. H. Lee, A. Matsuyama, and T. Sato, Phys. Rev. Lett. **104**, 042302 (2010).
[61] R. L. Workman *et al.* (Particle Data Group), Prog. Theor. Exp. Phys. **2022**, 083C01 (2022)
[62] M. Ablikim *et al.* (BES Collaboration), Phys. Rev. Lett. **97**, 062001 (2006).
[63] H. P. Morsch *et al.*, Phys. Rev. Lett. **69**, 1336 (1992).
[64] H. P. Morsch and P. Zupranski, Phys. Rev. C **61**, 024002 (1999).
[65] M. Bashkanov, H. Clement, and T. Skorodko, Nucl. Phys. A **958**, 129 (2017).
[66] M. Bashkanov, H. Clement, and T. Skorodko, Eur. Phys. J. A **51**, 87 (2015).
[67] G. Fäldt and C. Wilkin, Phys. Lett. B **701**, 619 (2011).
[68] M. Albaladejo and E. Oset, Phys. Rev. C **88**, 014006 (2013).
[69] Internal report, WASA-at-COSY (unpublished).
[70] V. I. Kukulin *et al.*, Phys. Lett. B **801**, 135146 (2020).
[71] G. Höhler, πN Newslett. **9**, 1 (1993).
[72] P. Adlarson *et al.*, Phys. Rev. C **102**, 015204 (2020).
[73] H. Rohdjeß *et al.*, Eur. Phys. J. A **18**, 555 (2003).
[74] SAID partial-wave solutions, http://gwdac.phys.gwu.edu.
[75] V. I. Kukulin *et al.*, Ann. Phys. **325**, 1173 (2010).
[76] V. I. Kukulin, V. N. Pomerantsev, O. A. Rubtsova, M. N. Platonova, and I. T. Obukhovsky, Chin. Phys. C **46**, 114106 (2022).